Screen Printed Moisture Sensor and Its Application on Smart Packaging

Ruoxi Ma[1], Alexandra Pekarovicova[2]

Keywords: barrier coating, food packaging, glucomannan, nano-fibrillated cellulose, SBS board, screen printing, moisture sensor

Abstract

The hemicellulose-based suspension with nano-fibrillated cellulose (NFC) composite film exhibit outstanding air barrier properties, which supports their applications as bio-based and biodegradable barrier coating on food packaging materials. The hydrophobic property of the hemicellulose-based biopolymer has been greatly improved (MVTR decreased by 49.7%) with crosslinking by using citric acid.

In this work, the crosslinked bio-polymer suspension was applied on solid bleached sulphate (SBS) board with a Meyer rod. Interdigitated electrodes were designed as moisture sensors and then screen printed on the coated SBS board with silver conductive ink. The hemicellulose-based barrier coating layer functioned as a moisture sensing layer. The printed sensor device was calibrated with its absorption and desorption isotherms at 23 °C with the range of relative humidity 20%-80%, followed by characterizations of the sensor's impedance change with each moisture level ranging from RH 20% to 80%. The breakthrough time was observed for each level of RH by measuring impedance using the LCR meter.

These findings point to the opportunity of coupling the hemicellulose-based barrier coatings with printed moisture sensors in order to boost their capabilities as smart barrier packaging materials.

Introduction

Flexible polymers are widely used in a multitude of food packaging applications, ranging from potato chips to take-away food wrappings. The current packaging industry strongly relies on petroleum-derived barrier films with production

[1]California Polytechnic State University; [2]Western Michigan University

processes contributing to the emission of greenhouse gases. Moreover, a majority of consumer packages go to landfill after a short usage life, which leads to environmental issues and sustainability limitations.

Polysaccharides that are used for packaging are chitosan, starches, cellulose and hemicellulose. They are nontoxic, widely used and available in the market also as waste materials. With great gas, aroma and grease barrier properties, such coatings have great potential in packaging materials. However, because of their hydrophilic nature, polysaccharides exhibit poor water vapor barriers [1,2]

Barrier coating layers for paper and board are commonly applied as dispersions or solutions. In the case of hemicellulose-based barrier polymers, the preparation of the dispersions often requires the use of citric acid to crosslink the polymer chains in order to form a three-dimensional network, which will improve the water resistance of the coating.

Porous cellulose-based materials, such as paperboard, have a great impact in the packaging industry due to their eco-friendly nature and biodegradability. However, hydrophilic behavior and a porous structure has limited the use of paper in a wide range of packaging applications. In order to overcome this issue, paper or paperboard is usually coated with a polymers or metal layer such as plastic or aluminum, to provide improvements in barrier properties at the expense of their eco-friendly and biodegradable nature [3].

Therefore, researchers are working to improve the moisture barrier property of the polysaccharides in order to broaden their potential applications on packaging materials. One way to increase the flexibility of the hemicellulose coating is to reduce the amount of hydrogen bonds using plasticizers, such as sorbitol [4] or glycerol [5,6]. These plasticizers have been shown to increase the tensile strength [7,8] and the oxygen barrier of films.

Another method to improve the dimensional stability and increase the hydrophobicity of coatings is through chemical cross-linking (esterification). The cross-linking procedure consists of the functional modification of the NC without its disintegration [9]. Different chemicals, such as toluenesulfonic acid, hexanoic acid [10], butyryl, benzoyl, naphtoyl, diphenvl acetatyl, and stearoyl [11] have been used to carry out this chemical crosslinking. However, poly (carboxylic acids) such as citric acid [12] or succinic acid [13] have become very popular because of their environmentally friendly and non-toxic nature. The cross-linking technique has also been used to improve the wet strength of cellulosic materials and to decrease the solubility in water of polysaccharides [14].

In our earlier study, barrier films based on hemicellulose, NFC and plasticizers were formulated [15]. Their mechanical strength (tensile properties), surface

properties (contact angle and surface energy, and PPS smoothness) and printability (print density). Then the strongest formulation of the stand-alone film was chosen to be crosslinked with citric acid in order to improve their strength and barrier properties. We evaluated the air permeability and water vapor transmission rate of the crosslinkable films against several benchmarks [16]. It is observed that given the same thickness of films, the MVTR, tensile properties and insoluble matter of the crosslinked formulations surpassed the film formulations without citric acid crosslinking. These positive results encourage the further development of crosslinkable glucomannan-based barrier coating formulations with respect to their industrial applications in roll-to-roll coating processes and smart packaging applications with printed electronics.

In this study, the barrier coating suspensions are formulated based on the crosslinked formulation of the hemicellulose-based film. An aqueous dispersion of the barrier coatings was prepared. The most promising formulations were coated onto commercial SBS board with Meyer rods, and the water vapor transmission rate (WVTR) and air permeability were characterized.

It is known in the food industry that a large amount of food is wasted during the transportation chain each year. Accurate monitoring and controlling of the environmental conditions imposed on perishable goods throughout transportation could optimize the transportation chain, yielding a reduced waste. Currently, it is already possible to envisage new applications related with smart packaging for perishable goods through printed electronics. Due to their potential low cost per surface area, mechanical flexibility and possibility of large scale processing [17,18] printed electronics encourage new opportunities in the field of sensing and electronics such as distributed sensing applications at large scale or monitoring of a high number of items in parallel. It has been reported of research in humidity capacitive-based sensors on plastic films [19]. An important part of these sensors utilizes the ability of certain polymers to absorb humidity, which will modify their dielectric properties. A type of micro sensor has been developed using gold patterned on parylene, and polyimide as the sensing layer [20]. Polyimide has also been used as substrate material for ultra-thin flexible chemical capacitive sensors in 2009 [21].

Resistive type humidity sensors contain noble precious metal electrodes either deposited on a glass or ceramic substrate by thick film printing techniques [22] or thick film deposition [23]. The design configuration of most resistive sensors is based on interdigitated electrodes [24] in which the humidity sensitive films are deposited in between them such that they touch the electrodes. The platform substrate can be coated either with electrolytic conductive polymers such as slats and acids [25, 26] or doped ceramic sensing films [27, 28]. In some cases, the film-based sensors are formed by applying screen printing and coating techniques such as spin coating and dip coating.

Resistive sensors measure the change of the humidity and translate it into a change in electrical impedance of the hygroscopic medium. Typically, the change of resistance to humidity follows an inverse exponential association, and almost varies from 1 KΩ to 100 MΩ. As a principle, upon adsorption of water vapor its molecules are dissociated to ionic functional hydroxyl groups and this results in an increase of film electrical conductance.

In this study, the hemicellulose-based barrier coating was applied on to back side of the commercial SBS board, and on top of it was screen printed moisture sensor. The devices that can sense the moisture change are interdigitated electrodes capacitors as depicted in figure.1 (a). It allows direct interaction between the sensor and the surrounding atmosphere. The primary design of the electrode capacitors included 20 paris of planar electrodes of 7mm length each, occupying a total surface area of 10mm x 4mm.

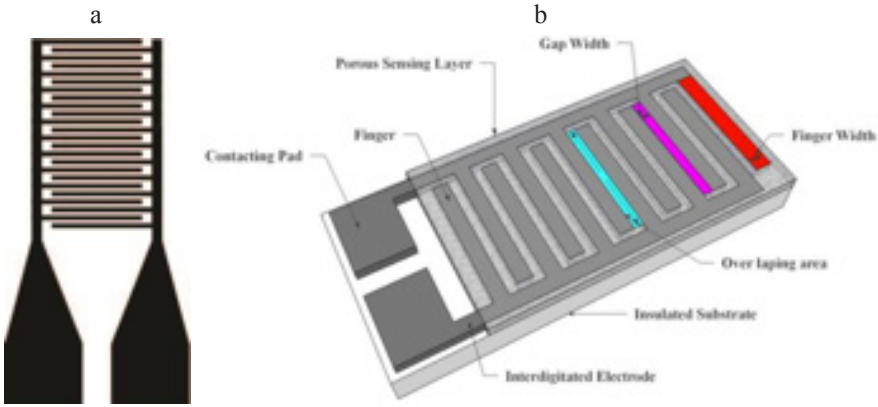

Figure 1: *The design interdigitated electrode (a) and its detailed structure (b) [29]*

The moisture sensor is based on the ability of certain structures to shift its capacitance and resistance in the presence of a target humidity level [30]. The interdigitated electrodes capacitors generate an electric field in both the dielectric layers underneath and on top of the electrodes plane. The layer underneath the electrodes will be referred as the substrate of the device. In this study, the substrate is SBS board which provides mechanical support. The hemicellulose-based barrier coating that functions to absorb the moisture vapor is called the sensing layer.

The water vapor is ideally adsorbed and absorbed in the coating layer. As a result, the sensing layer swells (increasing thickness) and its dielectric constant ε changes, modifying the value of C. The thicker the sensing layer is, the larger the amount of water molecules it can absorb under a fixed humidity level.

The aim of this study is to develop flexible packaging films [15] and coatings that are based on biodegradable, biocompatible and recyclable materials including nano-fibrillated cellulose and glucomannan. These films and coatings are aiming

to provide competitive barrier properties and ultimately leading to re-pulpable and biodegradable materials for packaging applications.

Experimental

Materials

Glucomannan from NOW Foods, Inc. in powder form was used. It was derived from the root of Amorphophallus konjac (Konjac plant). It is a glucose-mannose polysaccharide in which 5-10% of the sugars are acetylated. The molecule is structurally related to glucomannan from guar gum. Macroscopically, Konjac glucomannan is a soluble, fermentable, and highly viscous fiber.

Nano-fibrillated cellulose, (NFC, contains: water 95%-99%, cellulose pulp 1-5%; manufactured by the Department of Chemical and Biological Engineering, University of Maine Process Development Center) in a suspension form, was employed in this study. The sample was prepared mechanically by using a pilot scale refiner to break down the wood fibers. The wood fibers were a bleached softwood Kraft pulp. The suspensions were obtained at around 6.5% solids.
Sorbitol in powder form with a purity of 99%, from Sigma Aldrich. Citric Acid and Sodium Hypophosphite (SHP) from Sigma Aldrich in powder form with a purity of 98% were employed.

Coating Formulation

The hemicellulose-based barrier coatings are formulated based on the best stand-alone film formulation (CA25-C) in terms of their barrier property against moisture (characterized by MVTR). [16]

Component [g]	NFC [g]	Glucomannan [g]	Xylitol [g]	Citric Acid [g]	SHP* [g]
CA25-C	0.4	1	2	0.25	0.125

*Sodium Hypophosphite as catalyst

Table 1. *The crosslinking barrier coating formulation*

The prepared dispersion was coated on 266 g/m2 SBS board on laboratory scale. The coating was performed with a Meyer rod #46 that is capable of producing a 11.6 mm wet film thickness. The coated board samples were dried in the standard conditioning laboratory with 23 °C, RH 50% for 24 hours. The coating and drying processes were repeated 5 times in order to get significantly improved barrier properties. The barrier property was characterized by MVTR using the gravimetric method according to the ASTM E96 desiccant method.

Calendering and Conditioning of Samples

The coated samples were calendered at pressure of 25psi, 2-nip smooth side. The PPS roughness of the calendered samples are under 3 microns. All calendered samples were conditioned for 24 h at 50% RH and 25 °C before any measurements were made.

Sensor Printing

The interdigitated electrodes were printed on the hemicellulose-based barrier coated SBS board by using a precise screen printer (MSP-485 Affiliated Manufacturing Inc.) with silver conductive ink (AG-800 Applied Ink Solutions). A stainless steel screen, fabricated at Microscreen® with 325 mesh count, wire diameter of 28 μm, mesh angle of 22.5˚[31]. The printed electrodes have an initial resistance of 18.5±0.6 MΩ due to poorly connected silver particles, and resistance is decreased through sintering, which is a process that enhances junctions among particles and reduces resistivity. High temperatures can, for example, cause sintering by evaporate solvent and binders, which cause neck formation and particle growth that reduces a printed electrode's resistivity. The printed sensors were placed in an oven at 130 °C for 5 min in a VWR 1320 temperature control oven to thermally cure and sinter the conductive ink.

Sensor Calibration

The response of the impedance sensors was tested against changes in the humidity level from 20% to 80% RH at a constant temperature of 25 ºC. For this purpose, the printed moisture sensors were placed in the conditioning laboratory for 24 hours at 25 ºC and 50% RH. An uncoated SBS board was also conditioned and tested as control sample. Then the devices were put in a Thermotron® SE 1000 environmental chamber, which allowed for the automatic control of wet and dry airflow inside the cell at various temperature of choice. The chamber is equipped with an 8800 Data Acquisition (DAQ) system for controlling, monitoring, graphing and reporting environmental chamber data. The printed electrode was connected to an LCR meter (Agilent E4980a Precision) through wires and was put in the chamber with 20% RH without any sealed desiccant cup. The LCR meter was controlled by a custom-built LabVIEW™ program on the PC and used to record the impedance response of the printed sensor at an operating frequency of 1 kHz and an applied voltage of 1 V (Figure 2). The LCR-meter was used to measure the corresponding impedance values at a frequency of 1 kHz after the relative humidity and temperature reached stable values. Impedance and time measurements were controlled and recorded through a PC. Post-measurements data treatments were carried out with a PC to obtain differential values of impedance. This testing process served to equilibrate both sides of the sensor with moisture, providing a reliable base point that can be compared with the uncoated SBS board, hence evaluate the barrier property of

the coated SBS board. When observed the impedance reaching a constant level, it indicates that the sample has reached an equilibrium. Then the humidity level was increased from 20% RH to 80% RH with 10% increasing intervals until seven basepoints were observed and collected.

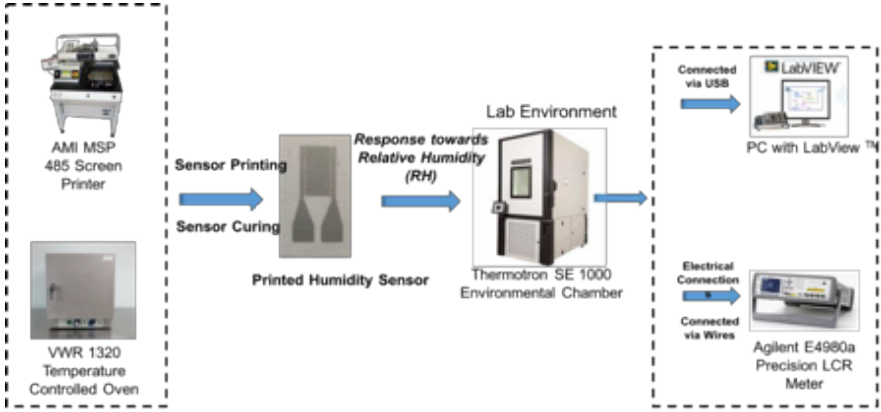

Figure 2: *The Experiment Setup for the IDE Humidity Sensor Printing and Characterizations.*

Result and Discussion

The objective of the sensor testing conducted in the humidity chamber was to identify if the hemicellulose-based coating layer on the SBS board is efficient to function as a barrier layer against moisture, hence be capable of being applied to food packaging materials for future use and further research development.

Barrier Properties Analysis

The barrier properties of the hemicellulose-based coated SBS board were characterized by correlating its coating thickness and coat weight versus its air permeability and MVTR (Table 2). The coating formulation was chosen according to the best stand-alone film formulation in regards to its MVTR value. The coated SBS board has a decreased air permeability coefficient by 2 orders of magnitude. Meanwhile, the barrier property characterized by moisture vapor transmission rate (MVTR) of the coated SBS board has been improved by 81.5%. Both the coat weight and coating thickness can be tuned by varying coating method, such as Meyer rods, depending on the end-use or application of the coated SBS board.

Sample	Caliper/ mm	Coating Thickness μm	Air Permeability Coefficient/μm^2	MVTR/g/m^2day	Coat Weight/g/m^2
SBS	0.353	n/a	$5.39x10^{-3}$	213.0	0
CA-C	0.371	18	$4.07x10^{-5}$	39.4	14.9

Table 2: *Barrier Properties of the Hemicellulose-based Coated Board.*

Humidity Sensor Response Analysis

The impedance humidity measurements were made in a humidity chamber (Thermotron® SE 1000) at a fixed temperature of 25ºC. The printed sensors on both coated and uncoated SBS boards were tested under a wide humidity range from 20% to 80% RH in 2-hour intervals. The humidity levels were set up in this interval due to the physical constraints of the humidity chamber. The selected time period was set up to 2 hours in order to allow the diffusion of water vapor molecules to be absorbed into the substrate and stabilized, reaching the equilibrium with the environment.

The output signals of both sensors were normalized to the nominal values of capacitance C_0 and resistance R_0. The real and the imaginary part of the sensor impedance are recorded during step- wise changes between 20% to 80% RH in 2 hour intervals. Stable humidity conditions are typically achieved within less than 15 minutes. The humidity equilibrates to stable levels with a small remaining drift (Figure 3). The real Z' and imaginary Z" of the complex paper-based sensor impedance (Z= Z'+iZ", where i = √-1) is recorded with test frequency of 1 kHz.

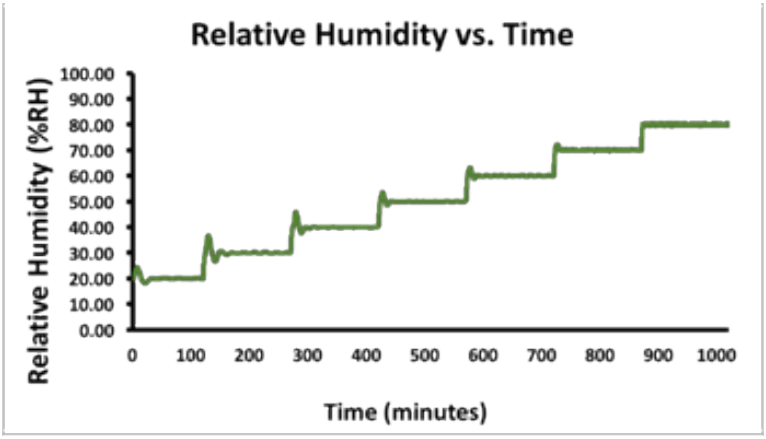

Figure 3: *The Stepwise Change of the Relative Humidity in the Test Chamber.*

Figure 4 shows the dynamic capacitance response of the sensor printed on the uncoated SBS board. The capacitance of the sensor printed on uncoated SBS board stepwise increased, corresponding with the increasing relative humidity in the chamber.

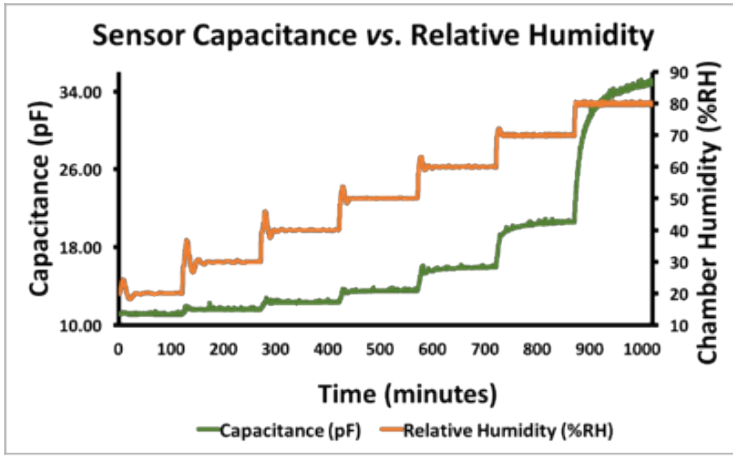

Figure 4: *Capacitance vs. RH Plot of Sensor Printed on Uncoated SBS Board.*

Figure 5 shows the dynamic capacitance response of sensor printed on the coated SBS board. The behavior shows a delaying of the sensor in the increasing RH intervals. This is due to saturation of the barrier coating functions as the sensing material. It can be explained by the adsorption process for the sensor when exposed to different relative humidity levels. The capacitance of the sensor printed on coated SBS board remains stable before the relative humidity in the chamber reached 75%. This behavior indicates the barrier coating layer successfully block out the moisture and delay the water vapor break through before 75% RH. Moreover, it can be observed from Figure 29 that at 80% RH, the capacitance of sensor printed on coated SBS board didn't reach equilibrium within the 2-hour interval. This indicates that at 80% RH, it will take more than 2 hours for the moisture vapor to break through the hemicellulose- barrier coating layer. In other words, the barrier property of the coating layer is shown to be significantly effective.

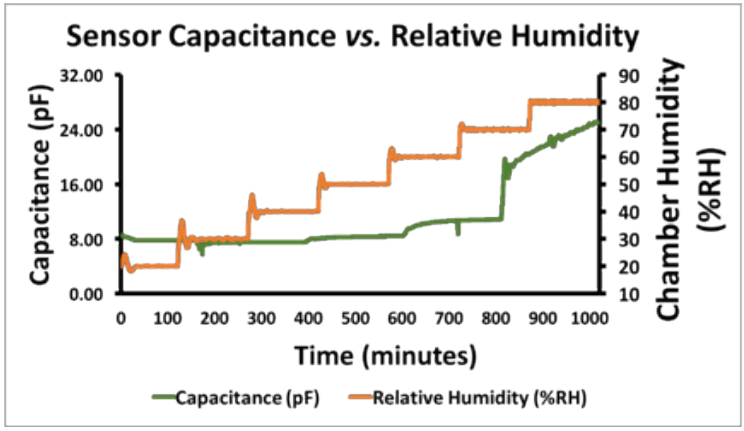

Figure 5: *Capacitance vs. RH Plot of Sensor Printed on Coated SBS Board.*

From the measurement data (capacitance and conductance) we are able to derive the sensor impedance using the equation (1)

$$R_x = \frac{1}{G_x}\ ; \quad Z = \frac{R_x}{1 + j\omega R_x C_x} \tag{1}$$

Where,
ω is the angular frequency;
ω=2πf; f=1 kHz.

The resistance on the coated SBS board also shows a delaying response (Figure 6), while for the uncoated SBS board, the resistance increases in stepwise correspondently with the increasing RH without hysteresis response (Figure 6).

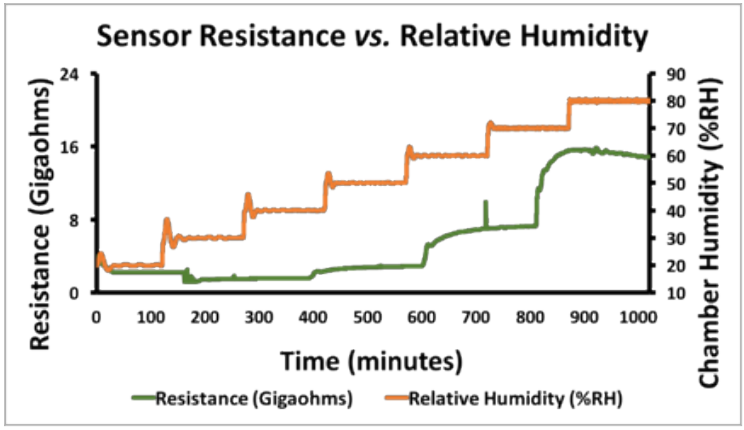

Figure 6: *Resistance vs. RH Plot of Sensor Printed on Coated SBS Board.*

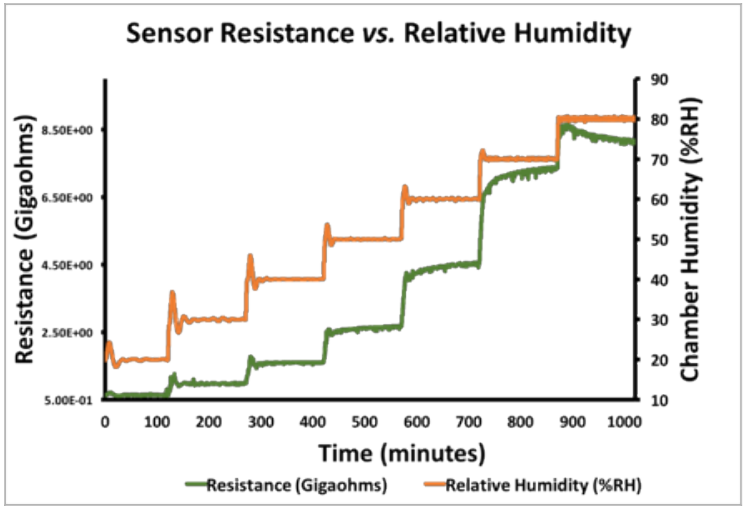

Figure 7: *Resistance vs. RH Plot of Sensor Printed on Uncoated SBS Board.*

In Figure 6 we can observe non-linear response of sensor printed on the hemicellulose-based barrier coated SBS board. It is very obvious that the resistance of the printed sensor remains stable around 3 Gohms from 20% to 50% RH. When the RH increased to 75%, resistance has a

breakthrough of 16 Gohms, indicating the dielectric constant of the coated SBS board was changed due to the total saturation of moisture vapor. In comparison, from Figure 7 we can observe the resistance response of the sensor printed on the uncoated SBS board increased stepwise with the increasing RH levels. Without any barrier coating, there is no delay in response.

Conclusion

A hemicellulose-based barrier coating was formulated and applied onto SBS board successfully. The barrier property has been characterized with its air permeability and moisture vapor transmission rate. A screen printed impedance humidity sensor was successfully designed, fabricated and tested. Tests were conducted in a humidity chamber by varying the relative humidity levels and measuring the changes in impedance. One of the objectives of this study-to develop a moisture and air barrier coating that can be applied in food packaging, has been fulfilled. Also, the impedance sensor printed on the coated and uncoated SBS boards has been analyzed at various RH levels. The impedance of the sensor increases with the increasing RH levels. However, the sensor printed on hemicellulose-based barrier coated SBS board delays the impedance increase until the RH reached 75%. This indicates that the hemicellulose-based barrier coating functions efficiently to block the moisture under low to moderate RH, hence possesses the potential to serve as liquid detector in moisture surveillance and tracking functions along the transportation and storage process.

Reference:

1. Zhang W, Xiao H and Qian L., Enhanced water vapor barrier and grease resistance of paper bilayer-coated with chitosan and beeswax. *Carbohydrate Polymers*, 2014. 101: p.401- 406.
2. Bordenave N, Grelier S and Coma V., Hydrophobization and Antimicrobial Activity of Chitosan and Paper-based Packaging Material. *Biomacromolecules*, 2010. 11: p. 88-96.
3. M., Tuomas Mehtio et al., Crosslinkable poly (lactic acid)-based materials: Biomass-derived solution for barrier coatings. *Journal of Applied Polymer Science*, 2016. 134: 44326.
4. Mathew A, Thielemans W and Dufresne A., Mechanical properties of nanocomposites from sorbitol plasticized starch and tunicin whiskers. *Journal of Applied Polymer Science*, 2008. 109: p. 4065-4074.

5. Xiao C, et al., Properties of regenerated cellulose films plasticized with a-monoglycerides. *Journal of Applied Polymer Science*, 2003. 89: p. 3500-3505.
6. Hansen N, Blomfeldt T, Hedenqvist M, Plackett D., Properties of plasticized composite films prepared from nanofibrillated cellulose and birch wood xylan. *Cellulose*, 2012. 19: p. 2015-2031
7. Liu X, et al., Regenerated cellulose film with enhanced tensile strength prepared with ionic liquid 1-ethyl-3-methylimidazolium acetate (EMI-MAc). *Cellulose*, 2013. 20:1391-1399.
8. Wang S., et al., Choline Chloride/urea as an effective plasticizer for production of cellulose films. *Carbohydrate Polymer*, 2015. 117: p. 133-139.
9. De Cuadro P., et al., Cross-linking of cellulose and poly (- ethylene glycol) with citric acid. *Reactive and Functional Polymers*, 2015. 90: p. 21-24.
10. Matsumura H., Sugiyama J. and Wolfgang G., Cellulosic nanocomposites. I. Thermally deformable cellulosic hex- anoates from heterogeneous reaction. *Journal of Applied Polymer Science*, 2000. 78:2242-2253.
11. Vuoti S., et al., Solvent impact on esterification and film formation ability of nanofibrillated cellulose. *Cellulose*, 2013. 20: p. 2359-2370.
12. Quellmalz A., and Mihranyan A., Citric acid cross-linked nanocellulose-based paper for size-exclusion nanofiltration. *ACS Biomaterials Science and Engineering*, 2015.1: p. 271-276.
13. Zhou Y. J., Luner P. and Caluwe P., Mechanism of cross-linking of paper with polyfunctional carboxylic acids. *Journal of Applied Polymer Science*, 1995. 58: p. 1523-1534.
14. Sirvio J., et al., Biocomposite cellulose-alginate films: promising packaging materials. *Food Chemistry*, 2014. 151: p. 343-351.
15. Ma R., Pekarovicova, A., Fleming, P. D., The preparation and characterization of hemicellulose-based printable films. *Cellulose Chemistry and Technology*, 2017. 51 (9-10): p. 939-948
16. Ma R., Pekarovicova, A., Fleming, P.D., Biopolymer Films from Glucomannan: The effects of Citric Acid Crosslinking on Barrier Properties. *Journal of Print Media Technology Research*, 2018. 1 (7): p.19-25.
17. Mäkelä, T., et al., Continuous roll-to-roll nanoimprinting of inherently conducting polyaniline. *Microelectronic Engineering*, 2007. 84 (5-8): p. 877-879.
18. Kololuoma T. K., et al., Towards roll-to-roll fabrication of electronics, optics, and optoelectronics for smart and intelligent packaging. *Proceedings of the SPIE 5363, Emerging Optoelectronic Applications*, 2004. p. 77.
19. Danick B., et al., Making environmental sensors on plastic foil. *Materials Today*, 2011. 14 (9): p. 416-423.
20. Lee C. Y., et al., Fabrication of micro sensors on a flexible substrate. *Sensors and Actuators A: Physical*, 2008. 147 (1): p.173-176.
21. Zampetti E., et al., Design and optimization of an ultra thin flexible capacitive humidity sensor. *Sensors and Actuators B: Chemical*, 2009. 143 (1): p. 302-307.

22. Traversa, E. et al., Environmental Monitoring Field Tests Using Screen-Printed Thick-Film Sensors Based on Semiconducting Oxides. *Sensors and Actuators B: Chemical*, 2000. 65: p.181-185.
23. Kunte, G. V.; Shivashankar, S.A. and Umarji, A.M., Humidity Sensing Characteristics of Hydrotungstite Thin Films. *Bulletin of Material Science*, 2009. 31: p. 835-839.
24. Mamishev, A. V., Sundara-Rajan, K. and Zahn, M., Interdigital Sensors and Transducers. *Proceedings of IEEE*, 2004. 92: p.808-845.
25. Moneyron, J. E., de Roy, A. and Besse, J. P., Realisation of a Humidity Sensor Based on the Protonic Conductor Zn2Al(OH)6ClnH2O. *Microelectronics International*, 1991. 8: p. 26-31.
26. Kim, E. et al., Colorimetric and Resistive Polymer Electrolyte Thin Films for Real-Time Humidity Sensors. *ACS Applied Materials & Interfaces*, 2012. 4: p. 5179-5187.
27. Wang, W. et al., Humidity Sensor Based on LiCl-Doped ZnO Electrospun Nanofibers. *Sensors and Actuators B: Chemical*, 2009. 141: p. 404-409.
28. Anbia, M. et al., Humidity Sensing Properties of the Sensor Based on V-Doped Nanoporous Ti0.9Sn0.1O2 Thin Film. *Chinese Journal of Chemistry*, 2012. 30: p. 842-846.
29. Hamid F., et al., Humidity sensors principle, mechanism and fabrication technologies: a comprehensive review. *Sensors*, 2014. 14 (5): p. 7881-7939.
30. Li Y., et al., Monolithic CMOS multi-transducer gas sensor microsystem for organic and inorganic analytes, *Sensors and Actuators B: Chemical*, 2007. 126 (2): p. 431-440.
31. Turkani S. V., et al, A carbon nanotube based NTC thermistor using additive print manufacturing processes. *Sensors and Actuators A: Physical*, 2018. 279: p.1-9.